Electronic Supplementary Material (ESI) for Lab on a Chip

Electronic Supplementary Information – ESI

Design of a prototype flow microreactor for synthetic biology *in vitro*

Christian R. Boehm, Paul S. Freemont* and Oscar Ces*

*to whom correspondence should be addressed: E. mail: p.freemont@imperial.ac.uk; o.ces@imperial.ac.uk

The supporting material includes:

(1) Kinetic enzyme characterisation in homogeneous solution
(2) Microfluidic chip design
(3) Coating of heparinised PDMS microchannels in avidin, Alexa Fluor 488 conjugate
(4) Modelling of a packed bed microreactor
(5) Absolute product yield of the model pathway immobilised *via* different strategies for biocatalyst compartmentalization
(6) Impact of Q and c_0(lactose) on specific conversion efficiency *in silico*
(7) Absolute product yield of the model pathway (single enzyme bead format) before and after optimisation of CE_n
(8) Fold-factor increase of specific conversion efficiency *in silico* and *in vitro*
(9) Cooperativity among optimised parameters *in silico*

(1) Kinetic enzyme characterisation in homogeneous solution

Enzyme	βGal		GOD		HRP	
Kinetic parameter	K_m *[mM]*	k_{cat} *[1 / s]*	K_m *[mM]*	k_{cat} *[1 / s]*	K_m *[mM]*	k_{cat} *[1 / s]*
pH 6.0	0.35 ± 0.10	277 ± 4.6	8.04 ± 1.51	347 ± 82	0.017 ± 0.0083	850 ± 89
pH 7.4	0.22 ± 0.042	500 ± 41	23.48 ± 4.08	24 ± 0.28	0.029 ± 0.0053	234 ± 8.5
pH 7.4 biotinylated	0.23 ± 0.032	215 ± 17	36.71 ± 0.13	18 ± 0.73	0.237 ± 0.0086	89 ± 15

Table S1: Kinetic enzyme characterisation in homogeneous solution. Shown are the kinetic parameters, Michaelis constants K_m and turnover numbers k_{cat}, individually determined for all model pathway enzymes in homogeneous solution.

ONPG assays of βGal, direct Amplex Red assays of HRP, and indirect Amplex Red assays of GOD were performed in SPB (50 mM Sodium phosphate buffer, plus 2 mM KCl, and 1 mM MgCl2, at pH 7.4) in triplicate at 28 °C.

(2) Microfluidic chip design

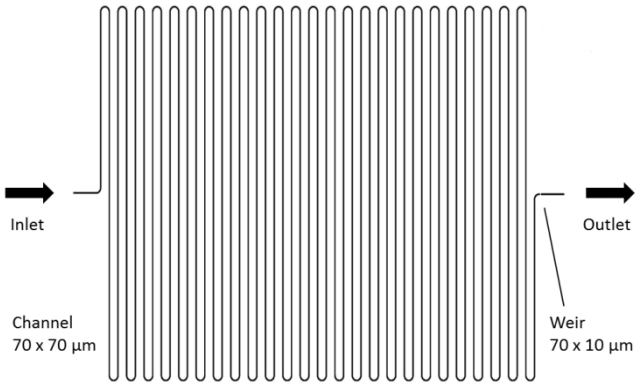

Fig. S2: Microfluidic chip design. Shown is a schematic representation of the microfluidic chip design employed for all continuous flow experiments performed within the scope of this work. 50 serpentines of a 70 x 70 µm microchannel connect the flow inlet to the outlet section, which features a 70 x 10 µm weir structure.

(3) Coating of heparinised PDMS microchannels in avidin, Alexa Fluor 488 conjugate

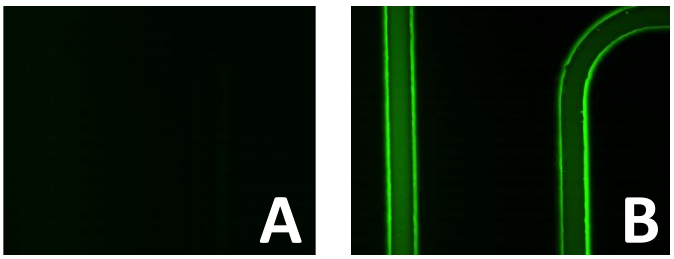

Fig. S3: Coating of heparinised PDMS microchannels in avidin, Alexa Fluor 488 conjugate. By contrast to a negative control lacking avidin (A), a heparin-treated PDMS microchannel coated in avidin, Alexa Fluor 488 conjugate (B) shows fluorescence stable to rinsing by more than five reactor volumes of buffer. Micrographs (480/535 nm) colored green were captured under 10 x magnification and 1000 ms exposure time.

(4) Modelling of a packed bed microreactor

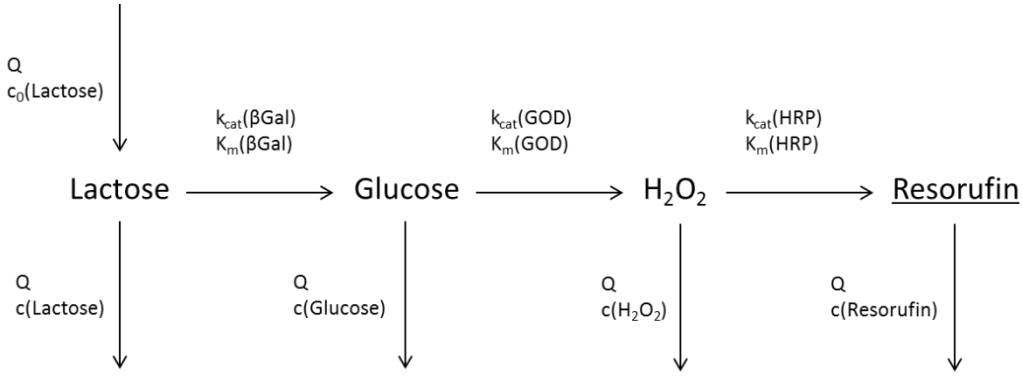

Fig. S4: Flow diagram of a packed bed microreactor model. Shown is a schematic flow diagram of a simple deterministic packed bed microreactor model in single enzyme bead format based on Michaelis-Menten kinetics. An initial concentration of the substrate c_0(lactose) is introduced at flow rate Q. The substrate is subsequently converted into resorufin due to sequential enzymatic action based on kinetic constants previously determined for the biotinylated pathway enzymes (see S1). As the microreactor represents a system under continuous flow, substrate, intermediates and product are constantly removed from the microcolumn via flow rate Q.

This system may be described using a set of simple ordinary differential equations (ODEs) as follows:

$$\frac{d[Lactose]}{dt} = \frac{Q \times c_0(Lactose)}{V} - [\beta Gal]\frac{k_{cat}(\beta Gal) \times [Lactose]}{K_m(\beta Gal) + [Lactose]} - \frac{Q \times [Lactose]}{V} \quad (i)$$

$$\frac{d[Glucose]}{dt} = [\beta Gal]\frac{k_{cat}(\beta Gal) \times [Lactose]}{K_m(\beta Gal) + [Lactose]} - [GOD]\frac{k_{cat}(GOD) \times [Glucose]}{K_m(GOD) + [Glucose]} - \frac{Q \times [Glucose]}{V} \quad (ii)$$

$$\frac{d[H_2O_2]}{dt} = [GOD]\frac{k_{cat}(GOD) \times [Glucose]}{K_m(GOD) + [Glucose]} - [HRP]\frac{k_{cat}(HRP) \times [H_2O_2]}{K_m(HRP) + [H_2O_2]} - \frac{Q \times [H_2O_2]}{V} \quad (iii)$$

$$\frac{d[Resorufin]}{dt} = [HRP]\frac{k_{cat}(HRP) \times [H_2O_2]}{K_m(HRP) + [H_2O_2]} - \frac{Q \times [Resorufin]}{V} \quad (iv)$$

Thereby, Q denotes the flow rate, V the reactor volume.

(5) Absolute product yield of the model pathway immobilised *via* different strategies for biocatalyst compartmentalisation

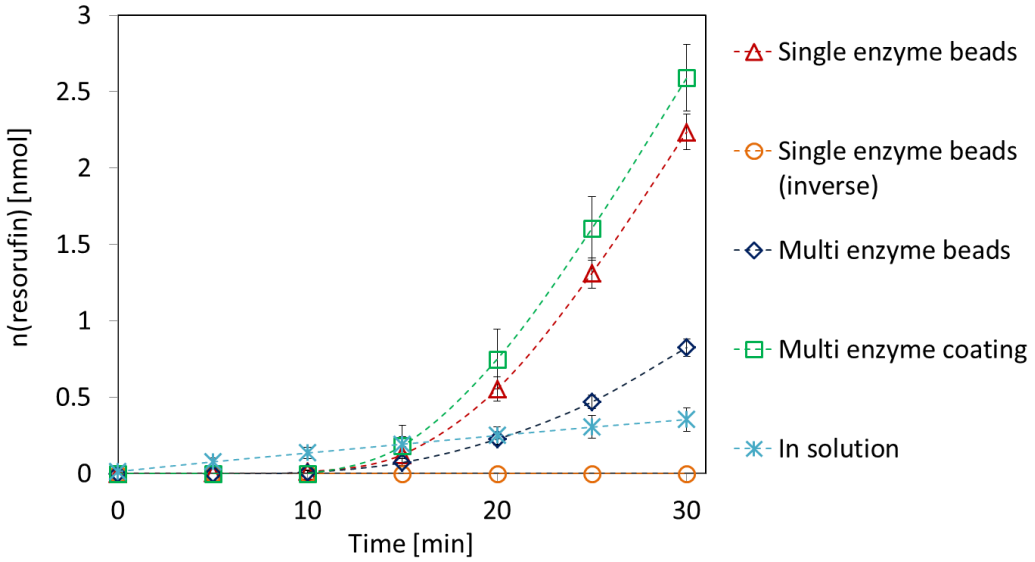

Fig. S5: Absolute product yield of the model pathway immobilised *via* different strategies for biocatalyst compartmentalisation. Continuous flow experiments were conducted at Q = 2.5 µl/min in presence of 100 mM lactose and 100 µM Amplex red in SPB. Total bead areas were A ~55.63 mm^2 at pathway composition C = 1:1:1 (n(βGal):n(GOD):n(HRP)) with a corresponding amount of biocatalyst applied for multi enzyme coating. Performance of the model pathway in homogeneous solution is shown as a reference.

(6) Impact of Q and c_0(lactose) on specific conversion efficiency *in silico*

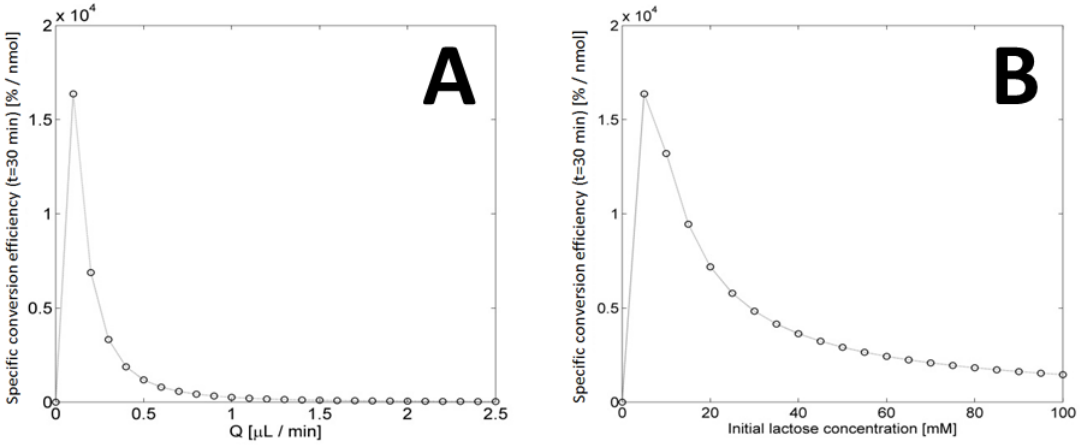

Fig. S6: *In silico* simulations showing the impact on specific conversion efficiency at t = 30 min for the model pathway immobilised via a packed bed microreactor (single enzyme bead format) resulting from variation of the individual parameters: (A) flow rate Q; (B) initial substrate concentration c_0(lactose). Other parameters are fixed at their suggested optimum values: Microcolumn composition C = 3:29:3 (n(βGal):n(GOD):n(HRP)); Total bead area A ~12.98 mm^2. Simulations over 30 min were performed with Q being varied from 0 to 2.5 µl/min in increments of 0.1 µl/min; c_0(lactose) being varied from 0 to 100 mM in increments of 5 mM.

(7) Absolute product yield of the model pathway (single enzyme bead format) before and after optimisation of CE_n

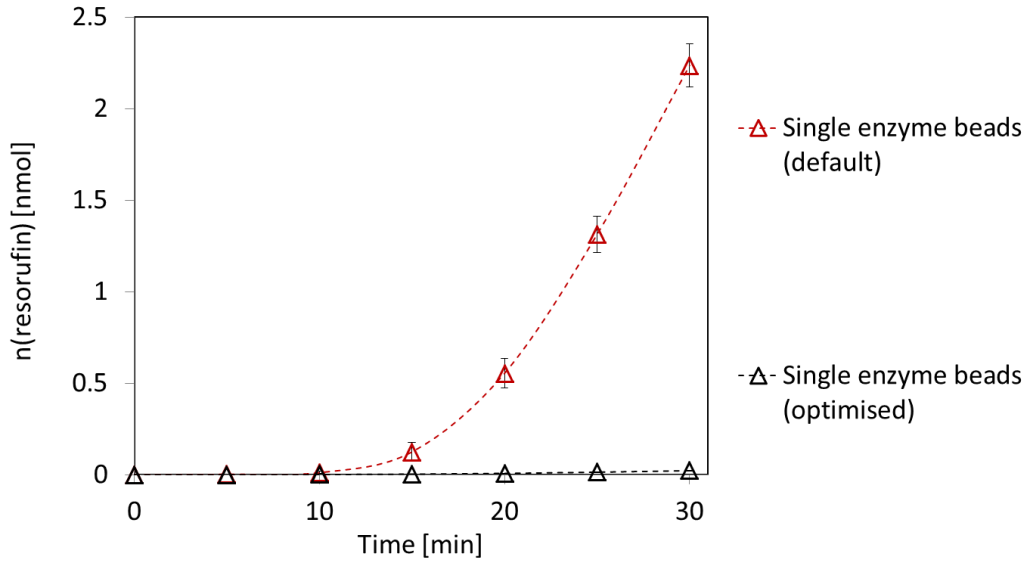

Fig. S7: Absolute product yield of the model pathway immobilised *via* a packed bed microreactor (single enzyme bead format) under default and optimised parameters for flow rate Q, initial substrate concentration c_0(lactose), microcolumn composition C, and total bead area A. Notably, parameters were optimized to maximise specific conversion efficiency CE_n, not total product yield.

(8) Fold-factor increase of specific conversion efficiency *in silico* and *in vitro*

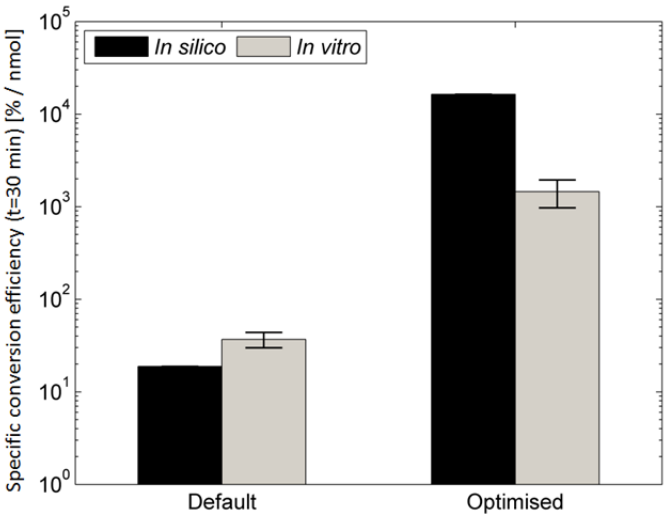

Fig. S8: Comparison of *in silico* and *in vitro* estimates of specific conversion efficiency at t = 30 min for the model pathway immobilised *via* a packed bed microreactor (single enzyme bead format) under the default and optimised parameter set, respectively.

(9) Cooperativity among optimised parameters *in silico*

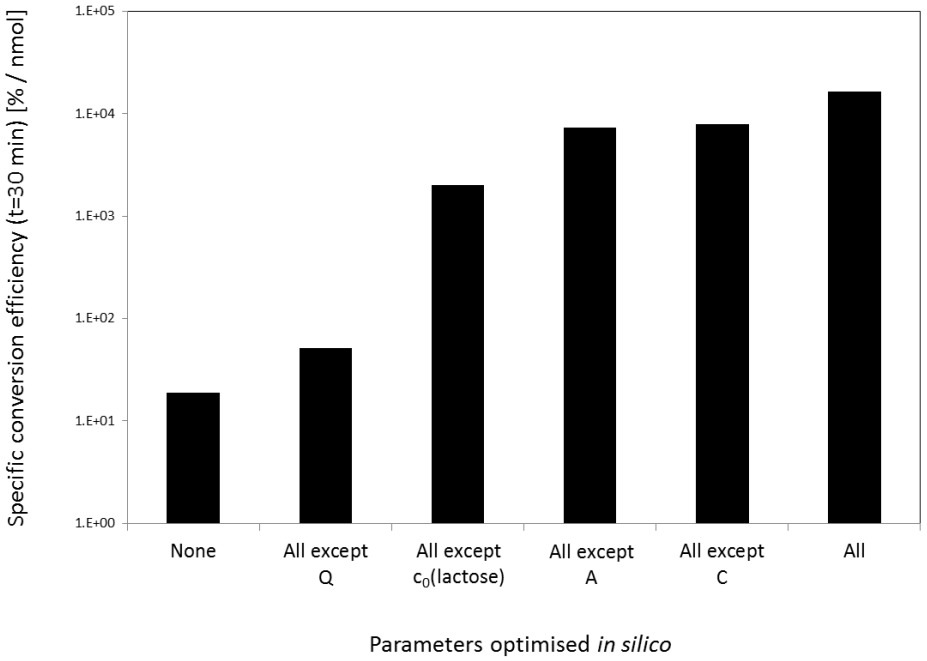

Fig. S9: Specific conversion efficiency of a packed bed microreactor (single enzyme bead format) predicted *in silico* at t = 30 min for various combinations of optimised / non-optimised parameters flow rate Q, initial substrate concentration c_0(lactose), microcolumn composition C, and total bead area A. Parameters not optimised equal their respective default values.